AIP Applied Physics Letters

Dual threshold diode based on the superconductor-to-insulator transition in ultrathin TiN films

Tatyana I. Baturina, David Kalok, Ante Bilušić, Valerii M. Vinokur, Mikhail R. Baklanov, Anton K. Gutakovskii, Alexander V. Latyshev, and Christoph Strunk

Citation: Applied Physics Letters **102**, 042601 (2013); doi: 10.1063/1.4789510
View online: http://dx.doi.org/10.1063/1.4789510
View Table of Contents: http://scitation.aip.org/content/aip/journal/apl/102/4?ver=pdfcov
Published by the AIP Publishing

APPLIED PHYSICS LETTERS **102**, 042601 (2013)

Dual threshold diode based on the superconductor-to-insulator transition in ultrathin TiN films

Tatyana I. Baturina,[1,2,3,a)] David Kalok,[2] Ante Bilušić,[2,4] Valerii M. Vinokur,[3]
Mikhail R. Baklanov,[5] Anton K. Gutakovskii,[1] Alexander V. Latyshev,[1] and Christoph Strunk[2]
[1]*A. V. Rzhanov Institute of Semiconductor Physics SB RAS, 13 Lavrentjev Avenue, Novosibirsk 630090, Russia*
[2]*Institut für experimentelle und angewandte Physik, Universität Regensburg, D-93025 Regensburg, Germany*
[3]*Materials Science Division, Argonne National Laboratory, 9700 S. Cass Avenue, Argonne, Illinois 60439, USA*
[4]*Faculty of Natural Sciences, University of Split, N. Tesle 12, HR-21000 Split, Croatia*
[5]*IMEC, Kapeldreef 75, B-3001 Leuven, Belgium*

(Received 1 October 2012; accepted 14 January 2013; published online 29 January 2013)

We investigate transport properties of superconducting TiN films in the vicinity of the superconductor-insulator transition (SIT). We show that the current-voltage (*I-V*) characteristics are mirror-symmetric with respect to the SIT and can be switched to each other by the applied magnetic field. In both superconducting and insulating states, the low-temperature *I-V* characteristics have pronounced diode-like threshold character, demonstrating voltage/current jumps over several orders of magnitude at the corresponding critical current or threshold voltage. We have found that for both states, the theory developed for Josephson junction arrays offers a quantitative description of the experimental results. © *2013 American Institute of Physics*. [http://dx.doi.org/10.1063/1.4789510]

The unique properties of titanium nitride (TiN) including its extreme hardness, high melting point, high thermal conductivity, high resistance to corrosion and wear and to atom diffusion within the matrix, make it an irreplaceable material for an incomparable wealth of applications in electronics. The excellent diffusion barrier characteristics of TiN are utilized in microcircuits.[1–3] TiN makes remarkable Schottky-barrier contacts to Si and GaAs suitable for high-temperature applications.[4–6] Furthermore, TiN possesses outstanding electrical properties for applications in thin film resistors in Π-type attenuators[7,8] and as transparent conductors.[9] TiN nanocrystal memory capacitors which enhance charge trapping properties of the charge trapping layer due to strong charge confinement in the TiN metal nanocrystals, are exceptional candidate for future nanoscale high-performance nonvolatile memory devices.[10,11] A diversity of TiN applications rests on the variety of deposition techniques,[12–20] such as dc, rf, magnetron sputtering, ion plating, activated reactive evaporation, laser physical vapour deposition, chemical vapour deposition, and atomic layer deposition (ALD), each targeting its specific application. What more, at low temperatures below $T_c = 6\,\mathrm{K}$, TiN turns superconducting, opening an important arena for applications and responding to the quest for high performance materials for ultrasensitive superconducting photon detectors.[21,22] The low temperature applications utilize remarkable tunability of thin superconducting TiN films, where the critical temperature and normal-state resistivity vary with composition.[23–25] Systematic studies of the low temperature transport properties of thin TiN films of the same composition revealed that the superconducting transition temperature decreases with the decrease of the film thickness d and/or with the increase of the normal state sheet resistance $R_\square$.[26–33]

The most recent finding was that ultrathin, $\lesssim 5\,\mathrm{nm}$, TiN films deposited by both reactive dc magnetron sputtering[30] and by ALD[34–36] may appear not only superconducting but, depending on $R_\square$, also *insulating*. Importantly, the transition between the superconducting and insulating states (SIT) in ultrathin TiN films can also be tuned by the magnetic field. The peculiarity of this insulating state is that it maintains superconducting correlations and is thus often referred to as the *Cooper-pair insulator*.

In this letter, we report our results on the low temperature studies on transport properties of superconducting TiN film which is on the verge of the superconductor-to-insulator transition. We show that the current-voltage (*I-V*) characteristics are strongly non-linear and have a threshold diode-like character at low temperatures. Furthermore, the *I-V* are symmetric with respect to the SIT and are switched to each other by the applied magnetic field.

As a starting material, we have chosen a 5 nm thin TiN film which was formed on a Si/SiO_2 substrate by the ALD at $T = 350\,°\mathrm{C}$. High resolution transmission electron microscopy (HRTEM) revealed the polycrystalline structure characteristic to stoichoimetric material with the densely packed crystallites of the average grain size of about 5 nm, the atomically smooth interface between the SiO_2 substrate and the TiN film, and the atomically smooth surface of the TiN film (Figs. 1(a) and 1(b)). Then the film was patterned by the conventional UV lithography and plasma etching into the bridges, the SEM image shown in Fig. 1(c). The initial as-grown film[33] has the room temperature sheet resistance $R_\square = 2.94\,\mathrm{k}\Omega$, resulting in resistivity $\rho = 1470\,\mu\Omega\cdot\mathrm{cm}$, the superconducting critical temperature $T_c = 1.115\,\mathrm{K}$, the diffusion constant $D = 0.3\,\mathrm{cm}^2/\mathrm{s}$, and the superconducting coherence length $\xi_d(0) = 9.3\,\mathrm{nm}$. Infrared studies[32] give plasma frequency $\omega_p = 3.17\,\mathrm{eV}$, and the zero-temperature superconducting gap $\Delta_0 = 0.22\,\mathrm{meV}$ is inferred from low-temperature scanning tunnelling spectroscopy measurements.[31] We have employed

[a)]Author to whom correspondence should be addressed. Electronic mail: tatbat@isp.nsc.ru.

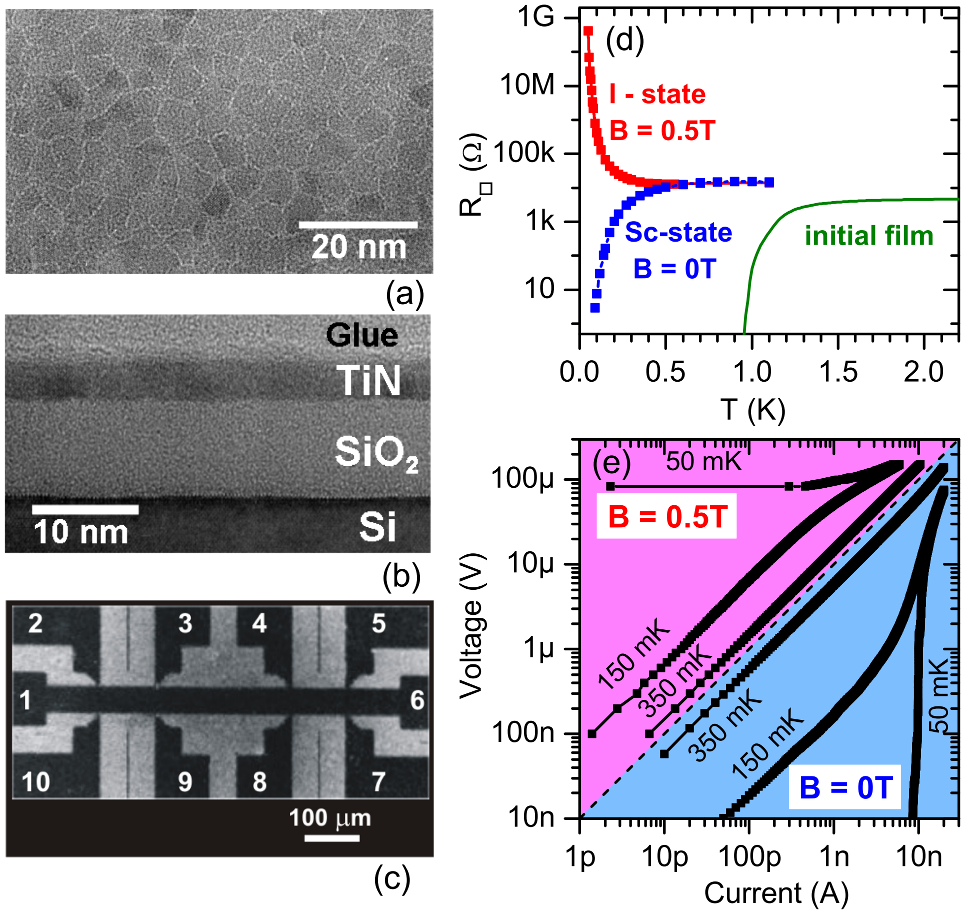

FIG. 1. High-resolution TEM images of the plan view (a) and the cross section (b) of the initial as-grown TiN film. (c) The SEM image of the sample. The black areas are the TiN film itself and the light grey areas are the etched parts. The numbers mark contact pads. The distance between the probes 2 and 5 is 450 μm and the sample width is 50 μm. It corresponds to nine squares at four-probe measurements, where the current flows between 1 and 6 contact pads. The area (accounting for a geometry factor) in two-probe measurements corresponds to 24 squares. (d) The resistance per square vs. temperature at zero magnetic field for the initial as-grown TiN film (solid line) and for the oxidized film at $B = 0$ T and $B = 0.5$ T, shown by symbols. (e) The representative dual current-voltage characteristics of the oxidized film at $B = 0$ T and $B = 0.5$ T at $T = 50$, 150, and 350 mK, the voltage axis showing voltages per square.

controlled oxidation in air at $T = 300\,^\circ$C to increase the room temperature film resistance up to $R_\square = 4.26\,\mathrm{k}\Omega$ in order to drive it to the very close proximity of the SIT.

Figure 1(d) shows the influence of the applied magnetic field on the film resistance in the linear response regime and demonstrates the magnetic field-driven SIT. Each data point of the $\log R_\square$ vs. T plots of Fig. 1(d) depicts a zero-bias resistance found from the dc I-V-characteristics measured by the four-probe technique in a low-resistive state and by the two-probe techniques in a high-resistive state. The contact resistances were negligible as was verified by comparing the two- and four-probe measurements. The used set ups enabled us to measure the resistances from 1 Ω up to 100 GΩ. Figure 1(e) shows the representative dual I-V characteristics in the log-log scale illustrating the mirror symmetry of superconducting and insulating sides of SIT. The curves are taken at three representative temperatures revealing three generic types of behaviour: (i) the ordinary Ohmic metallic response, $I \propto V$, at elevated temperatures (curves at $T = 350$ mK); (ii) linear low-drive response crossing over into the non-linear dependences upon increasing the applied voltage/current (curves at $T = 150$ mK); and (iii) switching behavior (curves at $T = 50$ mK).

Shown in Fig. 2 are $\log R_\square$ vs. $1/T$ plots for the representative magnetic fields. At zero magnetic field, the sample is superconducting with the resistance exhibiting the Arrhenius-like behaviour, $R_\square \propto \exp(-T_{J0}/T)$, over three orders of the magnitude. The dashed line presents the fit yielding $T_{J0} = 0.92$ K. Such a behaviour suggests that the dissipation mechanism is thermally activated phase slips. Employing the Ambegaokar-Halperin description of the phase diffusion through an overdamped Josephson junction,[38] we identify the activation energy as $k_B T_{J0} = 2E_{J0} = \hbar I_{c0}/e$, where E_{J0} is the Josephson coupling energy and I_{c0} is the zero-temperature Josephson critical current and find $I_{c0} \simeq 19$ nA. This value

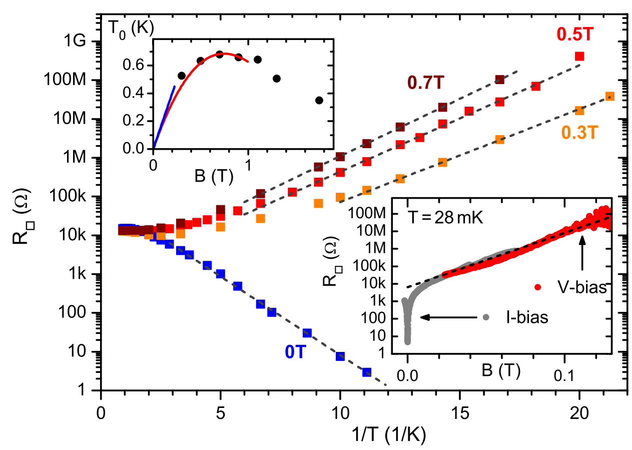

FIG. 2. $R_\square$ vs. $1/T$ at $B = 0$, 0.3, 0.5, and 0.7 T (symbols). Dashed lines show fits to the Arrhenius law. The bottom-right corner inset: matching of $R_\square(B)$ measured at $T = 28$ mK for the voltage and current bias setups, respectively. The current bias setup is realized by the four-probe ac lock-in technique, with the ac current of 40 pA and the frequency $f = 1.74$ Hz. In the two-probe voltage bias measurements, the ac voltage 4 μV and the same frequency were used. The dashed line corresponds to $R_\square(B) = R_0 \exp(B/B^*)$, with $B^* = 14$ mT and $R_0 = 6.45$ kΩ. The top-left corner inset: the activation temperature, T_0, as function of magnetic field B. The solid curve is the fit of $T_0(B)$ by Eq. (14) from Ref. 39. The straight line is the low-field tangent to the curve with the slope $T_0(B)/B = 2.0$ K/T.

remarkably compares with the independently measured low-temperature critical current $I_c \simeq 10$ nA. All the above is in accord with the expectations that SIT in a disordered film is of a percolative nature and that the electronic transport close to the transition is controlled by the phase diffusion over the saddle point critical junctions which couple superconducting clusters.[37]

The superconducting state in our film is fragile and is destroyed by extremely weak magnetic field perpendicular to the film: at $T = 28$ mK, the resistance $R_{\square}(B)$ shoots up over three orders of magnitude within the tiny interval from 0 to 5 mT, see the bottom-right corner inset in Fig. 2. Upon further increase of the field up to 0.1 T, $R_{\square}(B)$ grows exponentially, gaining another three orders of magnitude. This exponential growth can be expressed by formula $R_{\square}(B) = R_0 \exp(B/B^*)$. We have found $B^* = 14$ mT. The determined pre-exponential factor $R_0 = 6.45\,\mathrm{k}\Omega$ strikingly coincides with the quantum resistance for Cooper pairs, $h/(2e)^2$.

The resistance at finite fields exhibits the Arrhenius temperature behavior, $R_{\square}(T) \propto \exp(T_0/T)$. The magnitude and the non-monotonic magnetic field dependence of the activation energy T_0 shown in the top-left corner inset of Fig. 2 are in accord with the previously reported data on TiN films.[34–36] A change from the exponential decrease of the resistance at zero field to the mirror-symmetric exponential growth of the resistance with the decreasing temperature at finite fields demonstrates the duality between the superconducting and insulating behaviours of the critically disordered films not only in non-linear *I-V* curves but also in the linear response at both sides of the SIT. Applying the fitting procedure of $T_0(B)$ by Eq. (14) of Ref. 39 and taking into account the magnetic field dependence of the Josephson coupling energy for two-dimensional Josephson junction arrays in the nearest neighbors approximation,[40] we find $\Delta_c(0)/k_B = 2.05$ K, $A_{loop} = 0.98 \times 10^{-3} \mu\mathrm{m}^2$, and $\alpha E_J/E_c = 1$. Notably, at low magnetic fields, this fit gives the slope $\beta = T_0(B)/B = 2.0$ K/T (shown by the straight line in the top-left corner inset of Fig. 2), which, in its turn, immediately offers a quantitative expression for exponential growth of the resistance with the magnetic field in the low field region $R_{\square}(T, B) = R_0 \exp[\beta B/T]$. Indeed, earlier introduced B^* is equal to T/β determined independently from the linear approximation of $T_0(B)$, shown in the top inset of Fig. 2. This self-consistency in the description at both superconducting and insulating sides of the transition in terms of Josephson junction network physics is paralleled by the mirror-symmetric current-voltage characteristics of the artificially manufactured one- and two-dimensional Josephson junction arrays.[41–44] It is further interesting to note the similarities between the behavior of TiN films bordering the SIT and other materials, InO,[45–48] Be,[49] Ga,[50] to name a few (see also Refs. 51–53 for a review).

At low temperatures, the *I-V* characteristics acquire profoundly switching character both in the superconducting state (at I_c) and in the magnetic-field induced insulating state, where the current exhibits a jump at some threshold switching voltage V_T, see Fig. 1(e). At $T < 60$ mK, the value of V_T becomes stochastic and varies from one measurement to another. A random distribution of the threshold voltage is detrimental to applications.[54] Thus, it is important to understand the nature and borders of this behavior. To investigate the statistical distribution of V_T, we have repeatedly measured many *I-V* characteristics for each representative temperature and external magnetic field. Figure 3 displays the corresponding histograms of V_T at $B = 0.5$ T [panel a]; panels (b) and (c) show the temperature and the magnetic field dependences of the maximal and minimal values of V_T as well as indicate intervals containing 75% of the data. We observe that (i) the histograms have a sharp cut off at the maximal V_T; (ii) the most probable V_T is shifted towards the maximal value as temperature decreases. The above facts clearly evidence a non-Gaussian character of the V_T distribution and indicate the possible glassy character of the low-temperature state. (iii) The field-dependence of the most probable value of

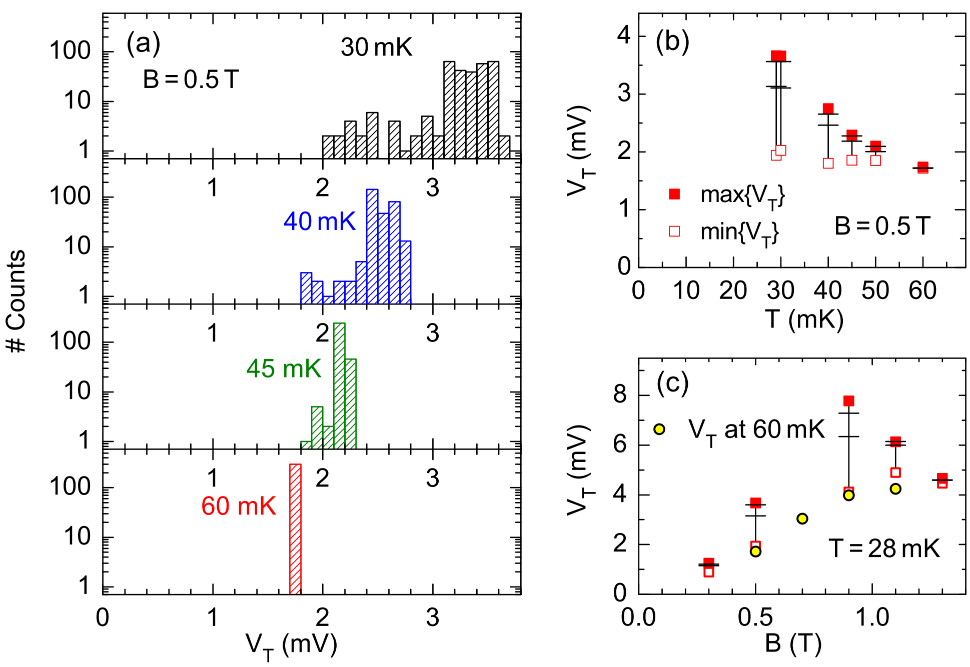

FIG. 3. Histograms for the V_T distribution: (a) $B = 0.5$ T and different temperatures (the samplings number at each temperature is 299); (b) and (c) Temperature (at $B = 0.5$ T) and field (at $T = 28$ mK) dependences of the variance range of V_T, maximal and minimal values shown by solid and open squares, respectively. Horizontal lines indicate intervals containing 75% of the data. V_T vs B at $T = 60$ mK is shown by circles in (c).

$V_T(B)$ is non-monotonic and has the values close to those observed on samples which are insulating at $B = 0$.[34] (iv) At $T < 45\,\text{mK}$, the ratio of $\max\{V_T(B)\}/\min\{V_T(B)\} \approx 2$ in magnetic fields below the field where the maximum of $V_T(B)$ is achieved, then it drops rapidly upon further field increase. (v) As the temperature grows, the ratio $\max\{V_T\}/\min\{V_T\}$ reduces to unity and the random scattering of V_T vanishes. Then at $T \geq 60\,\text{mK}$, the *I-V* characteristics become stable and fully reproducible, with V_T depending on the magnetic field. Stable and extremely sharp switching *I-V* characteristics at $T \gtrsim 60$ mK imply that in this temperature range, an ultra-thin TiN film can be used as a supersensitive sensor or a threshold detector.

To summarize, our findings break the ground for appealing applications of TiN in electronics. The specific property of our films is their ability to be in either of insulating, metallic, or superconducting states depending on their degree of oxidation and thickness. This enables the design of a whole circuit including all the above elements but cut out of the very same film, in particular, realizing the quantum circuits with the complementary architectures analogous to the conventional CMOS architectures in current electronics. Because of the sharpness of the threshold behaviour and the size of the current jump constituting several orders of magnitude, TiN films in the vicinity of superconductor-insulator transition hold high potential for becoming a base for sensors and detectors of unprecedented sensitivity and high useful signal-to-noise ratio. The dual character of threshold diode-like switching *I-V* characteristics opens routes for TiN films-based logical units which can be switched between two practically non-dissipative states by the magnetic field. Critically disordered TiN films constitute a single versatile platform for devices with dual operating characteristics and can be assembled to threshold detectors for either current or voltage transients. Another important application is photon detection, based on the photon-induced switching between insulating, resistive, and superconducting states.

The work was supported by the Deutsche Forschungsgemeinschaft under Grant No. 444USA113/3 and within the GRK 638, the Program "Quantum Mesoscopic and Disordered Systems" of the Russian Academy of Sciences, the Russian Foundation for Basic Research (Grant No. 12-02-00152), and the U.S. Department of Energy Office of Science under the Contract No. DE-AC02-06CH11357.

[1]M. Wittmer, Appl. Phys. Lett. **36**, 456 (1980).
[2]W. Sinke, G. P. A. Frijlink, and F. W. Saris, Appl. Phys. Lett. **47**, 471 (1985).
[3]S. N. Yoganand, M. S. Raghuveer, K. Jagannadham, L. Wu, A. Karoui, and G. Rozgonyi, Appl. Phys. Lett. **80**, 79 (2002).
[4]C. A. Dimitriadis, S. Logothetidis, and I. Alexandrou, Appl. Phys. Lett. **66**, 502 (1995).
[5]J. R. Waldrop, Appl. Phys. Lett. **43**, 87 (1983).
[6]J. Ding, Z. Liliental-Weber, E. R. Weber, J. Washburn, R. M. Fourkas, and N. W. Cheung, Appl. Phys. Lett. **52**, 2160 (1988).
[7]N. D. Cuong, S.-G. Yoon, D.-J. Kim, and B.-D. Kang, Appl. Phys. Lett. **90**, 183506 (2007).
[8]N. D. Cuong, S.-G. Yoon, and D.-J. Kim, Appl. Phys. Lett. **91**, 203502 (2007).
[9]M. Kiuchi and A. Chayahara, Appl. Phys. Lett. **64**, 1048 (1994).
[10]S. Choi, S.-S. Kim, M. Chang, H. Hwanga, S. Jeon, and C. Kim, Appl. Phys. Lett. **86**, 123110 (2005).
[11]S. Maikap, P. J. Tzeng, H. Y. Lee, C. C. Wang, T. C. Tien, L. S. Lee, and M.-J. Tsai, Appl. Phys. Lett. **91**, 043114 (2007).
[12]J. Narayan, P. Tiwari, X. Chen, J. Singh, R. Chowdhury, and T. Zheleva, Appl. Phys. Lett. **61**, 1290 (1992).
[13]B. W. Karr, I. Petrov, D. G. Cahill, and J. E. Greene, Appl. Phys. Lett. **70**, 1703 (1997).
[14]M. Boumerzoug, Z. Pang, M. Boudreau, P. Mascher, and J. G. Simmons, Appl. Phys. Lett. **66**, 302 (1995).
[15]A. Weber, R. Poeckelmann, and C. P. Klages, Appl. Phys. Lett. **67**, 2934 (1995).
[16]D.-H. Kim, S.-L. Cho, K.-B. Kim, J. J. Kim, J. Won Park, and J. J. Kim, Appl. Phys. Lett. **69**, 4182 (1996).
[17]M. Zeitler, J. W. Gerlach, T. Kraus, and B. Rauschenbach, Appl. Phys. Lett. **70**, 1254 (1997).
[18]Y. Fu, Y. T. Moon, F. Yun, Ü. Özgür, J. Q. Xie, S. Doğan, H. Morkoc, C. K. Inoki, T. S. Kuan, L. Zhou, and D. J. Smith, Appl. Phys. Lett. **86**, 043108 (2005).
[19]F. Fillot, S. Maîtrejean, I. Matko, and B. Chenevier, Appl. Phys. Lett. **92**, 023503 (2008).
[20]L. Wu, H. Y. Yu, X. Li, K. L. Pey, J. S. Pan, J. W. Chai, Y. S. Chiu, C. T. Lin, J. H. Xu, H. J. Wann, X. F. Yu, D. Y. Lee, K. Y. Hsu, and H. J. Tao, Appl. Phys. Lett. **96**, 113510 (2010).
[21]H. G. Leduc, B. Bumble, P. K. Day, B. Ho Eom, J. Gao, S. Golwala, B. A. Mazin, S. McHugh, A. Merrill, D. C. Moore, O. Noroozian, A. D. Turner, and J. Zmuidzinas, Appl. Phys. Lett. **97**, 102509 (2010).
[22]M. R. Vissers, J. Gao, D. S. Wisbey, D. A. Hite, C. C. Tsuei, A. D. Corcoles, M. Steffen, and D. P. Pappas, Appl. Phys. Lett. **97**, 232509 (2010).
[23]L. E. Toth, C. P. Wang, and C. M. Yen, Acta. Metall. **14**, 1403 (1966).
[24]W. Spengler, R. Kaiser, A. N. Christensen, and G. Müller-Vogt, Phys. Rev. B **17**, 1095 (1978).
[25]T. P. Thorpe, S. B. Qadri, S. A. Wolf, and J. H. Claassen, Appl. Phys. Lett. **49**, 1239 (1986).
[26]W. Tsai, M. Delfino, J. A. Fair, and D. Hodul, J. Appl. Phys. **73**, 4462 (1993).
[27]Y. Seguchi, T. Tsuboi, T. Kawahara, and T. Suzuki, J. Phys. Soc. Jpn. **64**, 4544 (1995).
[28]T. Suzuki, Y. Seguchi, and T. Tsuboi, J. Phys. Soc. Jpn. **69**, 1462 (2000).
[29]T. I. Baturina, D. R. Islamov, J. Bentner, C. Strunk, M. R. Baklanov, and A. Satta, JETP Lett. **79**, 337 (2004).
[30]N. Hadacek, M. Sanquer, and J.-C. Villégier, Phys. Rev. B **69**, 024505 (2004).
[31]B. Sacépé, C. Chapelier, T. I. Baturina, V. M. Vinokur, M. R. Baklanov, and M. Sanquer, Phys. Rev. Lett. **101**, 157006 (2008); Nat. Commun. **1**, 140 (2010).
[32]F. Pfuner, L. Degiorgi, T. I. Baturina, V. M. Vinokur, and M. R. Baklanov, New J. Phys. **11**, 113017 (2009).
[33]T. I. Baturina, S. V. Postolova, A. Yu. Mironov, A. Glatz, M. R. Baklanov, and V. M. Vinokur, EPL **97**, 17012 (2012).
[34]T. I. Baturina, A. Yu. Mironov, V. M. Vinokur, M. R. Baklanov, and C. Strunk, Phys. Rev. Lett. **99**, 257003 (2007).
[35]T. I. Baturina, A. Bilušić, A. Yu. Mironov, V. M. Vinokur, M. R. Baklanov, and C. Strunk, Physica C **468**, 316 (2008).
[36]T. I. Baturina, A. Yu. Mironov, V. M. Vinokur, M. R. Baklanov, and C. Strunk, JETP Lett. **88**, 752 (2008).
[37]E. Shimshoni, A. Auerbach, and A. Kapitulnik, Phys. Rev. Lett. **80**, 3352 (1998).
[38]V. Ambegaokar and B. I. Halperin, Phys. Rev. Lett. **22**, 1364 (1969).
[39]M. V. Fistul, V. M. Vinokur, and T. I. Baturina, Phys. Rev. Lett. **100**, 086805 (2008).
[40]M. Tinkham, D. W. Abraham, and C. J. Lobb, Phys. Rev. B **28**, 6578 (1983).
[41]L. J. Geerligs, M. Peters, L. E. M. de Groot, A. Verbruggen, and J. E. Mooij, Phys. Rev. Lett. **63**, 326 (1989).
[42]P. Delsing, C. D. Chen, D. B. Haviland, Y. Harada, and T. Claeson, Phys. Rev. B **50**, 3959 (1994).
[43]H. S. J. van der Zant, W. J. Elion, L. J. Geerligs, and J. E. Mooij, Phys. Rev. B **54**, 10081 (1996).
[44]E. Chow, P. Delsing, and D. B. Haviland, Phys. Rev. Lett. **81**, 204 (1998).
[45]G. Sambandamurthy, L. W. Engel, A. Johansson, and D. Shahar, Phys. Rev. Lett. **92**, 107005 (2004).
[46]G. Sambandamurthy, L. W. Engel, A. Johansson, E. Peled, and D. Shahar, Phys. Rev. Lett. **94**, 017003 (2005).

[47]M. Ovadia, B. Sacépé, and D. Shahar, Phys. Rev. Lett. **102**, 176802 (2009).
[48]O. Cohen, M. Ovadia, and D. Shahar, Phys. Rev. B **84**, 100507(R) (2011).
[49]E. Bielejec, J. Ruan, and W. Wu, Phys. Rev. B **63**, 100502(R) (2001).
[50]C. Christiansen, L. M. Hernandez, and A. M. Goldman, Phys. Rev. Lett. **88**, 037004 (2002).
[51]R. S. Newrock, C. J. Lobb, U. Geigenmüller, and M. Octavio, "The two-dimensional physics of Josephson junction arrays," Solid State Phys. **54**, 263 (1999).
[52]V. F. Gantmakher and V. T. Dolgopolov, Phys. Usp. **53**, 1 (2010).
[53]T. I. Baturina and V. M. Vinokur, "Superinsulator–superconductor duality in two dimensions," Ann. Phys. (published online); preprint arXiv:1209.0530.
[54]D. M. Kaplan, V. A. Sverdlov, and K. K. Likharev, Phys. Rev. B **68**, 045321 (2003).